AGU PUBLICATIONS

JGR

Journal of Geophysical Research: Biogeosciences

RESEARCH ARTICLE
10.1002/2013JG002525

Contribution no 14-118-J from the Kansas Agricultural Experiment Station.

Key Points:
- Large isotope disequilibrium was predicted at the site
- Models captured the dynamics leaf water isotope composition
- Precipitation was the main driver of the dynamics of flux isotope signatures

Supporting Information:
- Readme
- Figure S1

Correspondence to:
E. Santos,
esantos@ksu.edu

Citation:
Santos, E., C. Wagner-Riddle, X. Lee, J. Warland, S. Brown, R. Staebler, P. Bartlett, and K. Kim (2014), Temporal dynamics of oxygen isotope compositions of soil and canopy CO_2 fluxes in a temperate deciduous forest, *J. Geophys. Res. Biogeosci.*, *119*, 996–1013, doi:10.1002/2013JG002525.

Received 2 OCT 2013
Accepted 18 APR 2014
Accepted article online 29 APR 2014
Published online 31 MAY 2014

Temporal dynamics of oxygen isotope compositions of soil and canopy CO_2 fluxes in a temperate deciduous forest

E. Santos[1], C. Wagner-Riddle[2], X. Lee[3,4], J. Warland[2], S. Brown[2], R. Staebler[5], P. Bartlett[6], and K. Kim[3]

[1]Department of Agronomy, Kansas State University, Manhattan, Kansas, USA, [2]School of Environmental Sciences, Guelph, Ontario, Canada, [3]School of Forestry and Environmental Studies, Yale University, New Haven, Connecticut, USA, [4]Yale-NUIST Center on Atmospheric Environment, Nanjing University of Information, Science and Technology, Nanjing, China, [5]Air Quality Processes Research Section, Environment Canada, Toronto, Ontario, Canada, [6]Climate Processes Section, Environment Canada, Toronto, Ontario, Canada

Abstract Partitioning of CO_2 exchange into canopy (F_A) and soil (F_R) flux components is essential to improve our understanding of ecosystem processes. The stable isotope $C^{18}OO$ can be used for flux partitioning, but this approach depends on the magnitude and consistency of the isotope disequilibrium (D_{eq}), i.e., the difference between the isotope compositions of F_R (δ_A) and F_A (δ_R). In this study, high temporal resolution isotopic data were used (1) to test the suitability of existing steady state and nonsteady models to estimate $H_2{}^{18}O$ enrichment in a mixed forest canopy, (2) to investigate the temporal dynamics of δ_A using a big-leaf parameterization, and (3) to quantify the magnitude of the $C^{18}OO$ disequilibrium (D_{eq}) in a temperate deciduous forest throughout the growing season and to determine the sensitivity of this variable to the CO_2 hydration efficiency (θ_{eq}). A departure from steady state conditions was observed even at midday in this study, so the nonsteady state formulation provided better estimates of leaf water isotope composition. The dynamics of δ_R was mainly driven by changes in soil water isotope composition, caused by precipitation events. Large D_{eq} values (up to 11‰) were predicted; however, the magnitude of the disequilibrium was variable throughout the season. The magnitude of D_{eq} was also very sensitive to the hydration efficiencies in the canopy. For this temperate forest during most of the growing season, the magnitude of D_{eq} was inversely proportional to θ_{eq}, due to the very negative δ_R signal, which is contrary to observations for other ecosystems investigated in previous studies.

1. Introduction

Stable isotopes of CO_2, such as $^{13}CO_2$ and $C^{18}OO$, can be valuable tools to study the CO_2 exchange in a broad range of spatial scales [*Bowling et al.*, 2008; *Ogée et al.*, 2004; *Werner et al.*, 2012; *Yakir and Wang*, 1996; *Yakir and Sternberg*, 2000]. The partitioning of net ecosystem CO_2 exchange (F_N) into canopy (F_A) and soil (F_R) flux components is essential to improve our understanding of biophysical controls of photosynthesis and soil respiration processes at the ecosystem level. However, the success of the isotope flux partitioning approach depends on the magnitude and consistency of the isotope disequilibrium (D_{eq}), i.e., the difference between the isotope compositions of F_R (δ_A) and F_A (δ_R) [*Ogée et al.*, 2004; *Yakir and Wang*, 1996]:

$$D_{eq} = \delta_A - \delta_R \quad (1)$$

Larger ^{18}O D_{eq} values compared to ^{13}C D_{eq} are typically obtained in established ecosystems as the difference in ^{13}C composition of plant and soil sources is not very large [*Ogée et al.*, 2004], suggesting $C^{18}OO$ is a better tracer for partitioning F_N for these ecosystems. However, large temporal variability in ^{18}O D_{eq} has been observed in the few long-term studies conducted to date. *Wingate et al.* [2010] used automated branch chambers (for δ_A) and soil chambers (for δ_R) with continuous measurements of $C^{18}OO$ composition of the air using tunable diode laser spectroscopy (TDLS) and obtained typical daytime ^{18}O D_{eq} (denoted hereafter as D_{eq}) of 10‰ for a maritime pine stand; however, lower disequilibrium values were observed after rain events. *Griffis et al.* [2011] observed values of D_{eq} ranging from 0.3 to 17.1‰ for corn and also smaller D_{eq} values immediately after precipitation events using TDLS technique with soil chamber and eddy covariance measurements. Hence, longer-term studies to characterize the temporal dynamics of D_{eq} are needed.

The D_{eq} in ecosystems arise from the isotopic equilibration between CO_2 and water in soil and foliage, which usually have distinct $H_2{}^{18}O$ composition [*Yakir and Sternberg*, 2000]. The coupling between $\delta^{18}O$ of plant and soil CO_2 fluxes with their respective water pools requires prior knowledge of the isotope composition of water pools to interpret variations in δ_A and δ_R. Another important variable affecting δ_R is the rate of CO_2 hydration in soils, which has been reported to be faster than the uncatalyzed reaction in different ecosystems [*Griffis et al*., 2011; *Santos et al*., 2012; *Seibt et al*., 2006; *Wingate et al*., 2010; *Wingate et al*., 2009]. *Seibt et al*. [2006] hypothesized that the enhancement of CO_2 hydration was a result of the activity of the carbon anhydrase enzyme (CA) in the soil. The CA activity in soils and δ_R short-term variation [*Santos et al*., 2012; *Wingate et al*., 2010] can have important effects on D_{eq} and should be further investigated.

The leaf-level δ_A can be inferred directly from branch chambers [*Wingate et al*., 2010], but canopy-level δ_A cannot be measured directly and is usually estimated using big-leaf models [*Bowling et al*., 2001; *Lee et al*., 2009] or multilayer soil-vegetation-atmosphere transfer models [*Ogee et al*., 2003; *Ogée et al*., 2004]. The canopy-scale δ_A variation is driven by variables such as the efficiency of CO_2 hydration in the canopy, which is also dependent on CA activity in the foliage, canopy conductance, relative humidity, and the $H_2{}^{18}O$ composition of leaf water at the evaporation sites (δ_{Le}) [*Farquhar et al*., 1993]. This last variable is crucial for determining δ_A but cannot be measured directly at the canopy scale. However, the mechanisms governing δ_{Le} dynamics at the leaf scale are reasonably understood, and different models have been used to estimate leaf water $H_2{}^{18}O$ enrichment [*Craig and Gordon*, 1965; *Cuntz et al*., 2007; *Dongmann et al*., 1974; *Farquhar and Cernusak*, 2005]. The classic formulation proposed by *Craig and Gordon* [1965] to simulate the isotopic fractionation from a liquid water surface has been used to estimate δ_{Le} [*Dongmann et al*., 1974; *Flanagan et al*., 1991] by assuming steady state conditions, i.e., the water being transpired by the leaf has the same isotope composition of the water entering the leaf. Recent studies suggested that steady state conditions are often violated under field conditions [*Lai et al*., 2006; *Welp et al*., 2008; *Wingate et al*., 2010; *Xiao et al*., 2012]. *Farquhar and Cernusak* [2005] proposed a more detailed formulation, which takes into consideration the nonsteady state behavior and heterogeneity of leaf water isotope composition. There has been limited investigation of the effects of steady state versus nonsteady state models for δ_{Le} on δ_A for natural ecosystems over a growing season [*Griffis et al*., 2011; *Wingate et al*., 2010].

Models developed to estimate δ_{Le} use input variables measured near the leaf boundary layer [*Craig and Gordon*, 1965; *Farquhar and Cernusak*, 2005]. However, in canopy-scale studies, measurements are usually taken several meters above the canopy from which canopy-scale δ_{Le} and $H_2{}^{18}O$ composition of leaf bulk water (δ_{Lb}) can be derived through the application of a big-leaf model [*Lee et al*., 2009]. Recent research has shown that the isotope exchange is significantly affected by the intense turbulent mixing above plant canopies, which is negligible in the majority of chamber-based studies [*Griffis et al*., 2011; *Lee et al*., 2009; *Xiao et al*., 2012]. *Lee et al*. [2009] suggested that the inclusion of turbulent effects on the calculation of isotope kinetic factors through addition of an aerodynamic resistance might improve the estimates of regional and global isotope budgets. Furthermore, studies over crop canopies have shown that estimates of δ_{Lb} improved when turbulence effects were included in a big-leaf parameterization for isotope exchange [*Griffis et al*., 2011; *Xiao et al*., 2012]. However, additional investigation of the turbulence effects on canopy-scale $H_2{}^{18}O$ enrichment is required in forest ecosystems, where the magnitude of the aerodynamic resistance is much smaller than over crop canopies.

Lee et al. [2009] demonstrated that parameterized canopy-scale kinetic factors are more appropriate to study isotope CO_2 and water vapor exchange at the ecosystem level, when measurements are taken at a reference point above the canopy air space. Canopy-scale studies have also indicated that some parameters of leaf-scale models, such as the CO_2 hydration efficiency in the foliage, may not be scaled-up properly to the canopy level [*Griffis et al*., 2011; *Xiao et al*., 2012; *Xiao et al*., 2010]. *Xiao et al*. [2011] found that the canopy-scale CO_2 hydration efficiency (θ_{eq}), derived from eddy isoforcing measurements above a soybean canopy, was 0.46, which is much lower than the leaf-scale CO_2 hydration efficiency ($\theta_{eq} = 0.75$), obtained for C-3 plants under laboratory conditions [*Gillon and Yakir*, 2001]. Similar results were found by *Griffis et al*. [2011] who reported significantly smaller canopy-scale θ_{eq} for a corn canopy than that measured in laboratory conditions. How these contrasting canopy and leaf θ_{eq} values affect the ^{18}O D_{eq} derived using a big-leaf model is not clear.

Advances in optical techniques in recent years have allowed the development of analyzers capable of providing robust measurements of water and CO_2 isotopes under field conditions [*Griffis*, 2013]. Studies investigating the mechanisms controlling isotope exchange at the ecosystem scale and their temporal dynamics are needed [*Griffis et al*., 2011; *Xiao et al*., 2012; *Xiao et al*., 2010]. In this study, the biophysical processes governing canopy-scale isotope exchange in a forest ecosystem were investigated using detailed isotope measurements during a growing season. Atmospheric $C^{18}OO$ and $H_2{}^{18}O$ composition (δ_a and δ_v, respectively) were measured quasi-continuously and simultaneously above a temperate deciduous forest during a growing season using TDLS. In addition, detailed measurements of the $H_2{}^{18}O$ composition of ecosystem water pools were taken throughout the growing season. These measurements and additional supporting variables were used (1) to test the suitability of existing steady state and nonsteady state leaf enrichment models to estimate $H_2{}^{18}O$ enrichment of the foliage at the canopy scale in a mixed forest, (2) to investigate the temporal dynamics of δ_A using a big-leaf parameterization, which takes into account turbulence effects on isotope gaseous diffusion in plant canopies, and (3) to quantify the magnitude of D_{eq} in a temperate deciduous forest throughout the growing season and to determine the sensitivity of this variable to CO_2 hydration efficiency.

2. THEORY

2.1. $C^{18}OO$ Composition of Canopy CO_2 Flux

Lee et al. [2009] proposed a big-leaf parameterization to study land-air isotope fluxes, in which the $C^{18}OO$ exchange between plant canopy-atmosphere is an extension of previous leaf-scale formulations [*Farquhar et al*., 1993; *Flanagan et al*., 1991] and the isotope exchange pathways are described using a series of resistances. In this approach, the $C^{18}OO$ composition of the canopy flux (δ_A) is expressed as

$$\delta_A = \left[\frac{C_c}{C_c - C_a}(\delta_{Le} - \delta_a)\theta_{eq} + (1 - \theta_{eq})\varepsilon_{k,c}\frac{C_c}{C_a} - \varepsilon_{k,c}\right] + \delta_a \quad (2)$$

where C_a is the CO_2 molar density (μmol m^{-3}) in the air and δ_a is the air's $C^{18}OO$ composition measured above the forest canopy (section 3.2), C_c is the CO_2 molar concentration (μmol m^{-3}) in the chloroplasts, estimated using a physiological model (Appendix A), δ_{Le} is the canopy-scale $H_2{}^{18}O$ composition of the leaf water at the evaporative site (‰, VPDB scale), θ_{eq} is the extent of the CO_2 hydration in the canopy, and $\varepsilon_{k,c}$ is the CO_2 canopy-scale kinetic fractionation factor. The $\varepsilon_{k,c}$ takes into consideration the net fractionation of CO_2 during diffusion through the leaf boundary layer (5.8‰) and stomata (8.8‰) and was calculated using a resistance weighting method [*Lee et al*., 2009] as follows:

$$\varepsilon_{k,c} = \frac{5.8r_{b,c} + 8.8r_{c,c}}{r_a + r_{b,c} + r_{c,c}} \quad (3)$$

where r_a is the aerodynamic resistance and $r_{b,c}$ and $r_{c,c}$ are the boundary layer and canopy resistances for CO_2, respectively. The resistances r_a and $r_{b,c}$ were calculated using land surface modeling standard procedures following *Lee et al*. [2009] (equations (A8) and (A9)), and $r_{c,c}$ was estimated by scaling up the stomatal resistance (equation (A10)) obtained using the physiological model described in Appendix A.

We initially adopted a leaf-scale θ_{eq} of 0.96 derived for forest/shrub vegetation by *Gillon and Yakir* [2001] based on an extensive survey of CA activity and CO_2 exchange rate in species from the major plant groups. However, recent studies have found evidence that canopy-scale θ_{eq} values are much lower than the leaf-scale values [*Griffis et al*., 2011; *Xiao et al*., 2010]. *Xiao et al*. [2010] used measurements of $C^{18}OO$ isoforcing, obtained using the eddy covariance technique, to optimize θ_{eq} for a soybean canopy. They found that canopy-scale θ_{eq} was 0.46 for midday periods, which is much smaller than the leaf-scale default θ_{eq} of 0.75, observed under laboratory conditions [*Gillon and Yakir*, 2001]. *Griffis et al*. [2011] performed an optimization using isoflux measurements and found θ_{eq} of 0.196 for a corn canopy during the growing season. This value was significantly smaller than the average θ_{eq} (~0.70) determined for corn leaves at their site. To quantify the impact of θ_{eq} on D_{eq}, we also calculated δ_A using lower values of 0.25 and 0.6 for θ_{eq} in equation (2).

2.2. $H_2{}^{18}O$ Composition of Leaf Water

The foliage water isotope composition was simulated using two different formulations. The steady state formulation proposed by *Craig and Gordon* [1965] (CG, hereafter), with the assumption that the leaf water

pool is well mixed, so that the $H_2{}^{18}O$ composition at the evaporative site ($\delta_{Le,s}$) and bulk leaf water ($\delta_{Lb,s}$) are the same under steady state conditions (i.e., $\delta_{Le,s} = \delta_{Lb,s}$). The second formulation used in this study is the more sophisticated model developed by *Farquhar and Cernusak* [2005] (FC, hereafter), which takes into account nonsteady state conditions and the progressive $H_2{}^{18}O$ enrichment of leaf water as the water molecules move away from the xylem to foliar evaporative sites.

The CG model has been extensively used to calculate the $H_2{}^{18}O$ composition of leaf water at evaporative site [*Dongmann et al*., 1974; *Flanagan et al*., 1991; *Welp et al*., 2008; *Xiao et al*., 2012]. This formulation is based on the main assumption that transpiration is in isotopic steady state; i.e., the water leaving the leaf has the same isotope composition of xylem water (δ_x) entering the leaf. The $H_2{}^{18}O$ composition of leaf water under steady state conditions ($\delta_{Le,s}$) is given by

$$\delta_{Le,s} = \delta_x + \varepsilon_{eq} + \varepsilon_{k,w} + h\left(\delta_v - \varepsilon_{k,w} - \delta_x\right) \tag{4}$$

where $\varepsilon_{eq} = (1 - 1/\alpha_{eq})$, α_{eq} is the water equilibrium fractionation factor between liquid water and water vapor (> 0, ‰) [*Majoube*, 1971], h is the relative humidity at the canopy temperature, δ_v is the measured $H_2{}^{18}O$ composition of the air above the forest canopy (section 3.2), and $\varepsilon_{k,w}$ (‰) is the canopy-scale kinetic fractionation factor for vapor diffusion. The canopy temperature needed for derivation of h was estimated from outgoing long-wave radiation measured using a four-component net radiometer (section 3.3) and the Stefan-Boltzmann equation. The $\varepsilon_{k,w}$ was estimated, similarly to equation (3), following [*Lee et al*., 2009]

$$\varepsilon_{k,w} = \frac{21 r_{b,w} + 32 r_{c,w}}{r_a + r_{b,w} + r_{c,w}} \tag{5}$$

where $r_{b,w}$ and $r_{c,w}$ are the boundary layer and canopy resistances for H_2O, respectively, and are given by $r_{b,w} = 1.4 r_{b,c}$. and $r_{c,w} = 1.6 r_{c,c}$.

Farquhar and Cernusak [2005] proposed a formulation (hereafter FC) for situations in which the isotope composition of leaf transpiration may depart from steady state conditions and the leaf water pool is not necessary well mixed. In this formulation, the isotope composition of water at the evaporative site (δ_{Le}) and of the leaf bulk water (δ_{Lb}) for nonsteady state conditions are given by

$$\delta_{Le} = \delta_{Le,s} - \frac{\alpha_k \alpha_{eq} r_t}{w_i} \cdot \frac{\mathrm{d}\left(W \cdot \frac{1-e^{-P}}{P} \cdot (\delta_{Le} - \delta_x)\right)}{\mathrm{d}t} \tag{6}$$

$$\delta_{Lb} = \delta^P_{Lb,s} - \frac{\alpha_k \alpha_{eq} r_t}{w_i} \cdot \frac{1 - e^{-P}}{P} \cdot \frac{\mathrm{d}(W \cdot (\delta_{Lb} - \delta_x))}{\mathrm{d}t} \tag{7}$$

where α_k is the fractionation factor for diffusion ($\alpha_k = 1 + \varepsilon_{k,w}/1000$), $r_t = r_a + r_{b,w} + r_{c,w}$, w_i is mole fraction of (light) water in the intercellular space, P is the Péclet number, W is the foliage water content, and $\delta^P_{Lb,s}$ is described below. In this study, W was assumed to be constant and equal to 47.8 mol m^{-2}, which was the average W found for the foliage of a temperate mixed forest in northeastern United States [*Lee et al*., 2007]. Equations (6) and (7) were solved iteratively by changing the values of δ_{Le} and δ_{Lb} on the right-hand side until they matched the expressions on the left hand side.

The term $\delta^P_{Lb,s}$ in equation (7) represents the relationship between the isotope composition of bulk leaf water and water at the evaporative site as mediated by the Péclet effect [*Farquhar and Cernusak* [2005]:

$$\delta^P_{Lb,s} = \frac{\delta_{Le,s}\left(1 - e^{-P}\right)}{P} \tag{8}$$

The Péclet number represents the ratio of transpiration advection of unenriched xylem water to the diffusion of $H_2{}^{18}O$-enriched water from evaporating sites [*Farquhar and Lloyd*, 1993] and is given by

$$P = \frac{E_T L}{CD} \tag{9}$$

where L is the effective diffusion length derived using an optimization procedure, C (mol m^{-3}) is the density of liquid water and D is the temperature dependent diffusivity of $H_2{}^{18}O$ in water [*Cuntz et al*., 2007], and E_T is the transpiration rate of the foliage (mol m^{-2} s^{-1}) given by

$$E_T = \frac{\rho_a}{M_w} \frac{q(T_c) - q_a}{r_a + r_{c,w}} \tag{10}$$

where ρ_a is the air density, M_w is the water molar mass, $q(T_c)$ is saturation specific humidity at the canopy surface temperature (T_c), and q_a is the specific humidity at the reference height.

2.3. $C^{18}OO$ Composition of Soil CO_2 Flux

The $C^{18}OO$ composition of soil CO_2 flux was estimated using an analytical formulation [*Tans*, 1998; *Wingate et al*., 2009]. *Santos et al*. [2012] used this formulation to estimate δ_R at the same site and observed agreement with measured δ_R using the isotope flux ratio method near the forest floor. This formulation takes into consideration the different processes controlling the $C^{18}OO$ budget, such as $C^{18}OO$ production and diffusion in the soil and exchange of oxygen molecules between CO_2 and liquid water in the soil. These processes are described in the soil $C^{18}OO$ budget equation [*Amundson et al*., 1998; *Hesterberg and Siegenthaler*, 1991; *Tans*, 1998; *Wingate et al*., 2009]. Although *Santos et al*. [2012] conducted measurements of δ_R at the same site over the same time of year as this study, these measurements were not coincident in time (i.e., they were restricted to a few days a week). Hence, an analytical solution of the soil $C^{18}OO$ budget equation assuming steady state conditions and isothermal and uniform soil water conditions [*Wingate et al*., 2010; *Wingate et al*., 2009] was used to estimate δ_R. Although this is a simplification of field conditions, estimates of δ_R were in agreement with direct measurements of δ_R obtained using the isotope flux ratio method [*Santos et al*., 2012] at the site, providing confidence in modeled δ_R (‰, VPDB) values using the *Wingate et. al*. [2009] analytical formulation:

$$\delta_R = \delta_{\mathrm{eq},s} + \varepsilon_{d,\mathrm{eff}} + \left(\delta_{\mathrm{eq},s} - \delta_a\right) v_{\mathrm{inv}} \frac{C_a}{F_R} \tag{11}$$

where $\delta_{\mathrm{eq},s}$ (‰, VPDB) is the isotopic composition of CO_2 in isotopic equilibrium with the soil water, F_R (μmol m^{-2} s^{-1}) is the soil CO_2 flux, measured using soil chambers (as described in section 3.3), $\varepsilon_{d,\mathrm{eff}}$ is the effective isotopic fractionation during CO_2 diffusion in soil pores [*Wingate et al*., 2009], and v_{inv} (m s^{-1}) represents the rate at which oxygen atoms in CO_2 present in a column of air above the soil are exchanged with oxygen atoms in soil liquid water [*Tans*, 1998]. This term is given by $v_{\mathrm{inv}} = \sqrt{B\theta_w k_s D_{18}}$, where B is Bunsen's solubility coefficient for CO_2, and a function of soil temperature (T_s) ($B = 1.739 \times \exp(-0.0390 \times T_s + 0.000236 \times T_s^2)$ [*Weiss*, 1974], θ_w is the soil water content, and D_{18} is the effective diffusivity of $C^{18}OO$ in soil air. The k_s is the effective rate of oxygen exchange between CO_2 and liquid water given by

$$k_s = f_{CA} k_h \tag{12}$$

where f_{CA} is the relative increase in hydration resulting from activity of the CA enzyme in the soil [*Riley et al*., 2003; *Seibt et al*., 2006; *Wingate et al*., 2008] and k_h is the rate of oxygen isotope exchange between CO_2 and water, equal to $1/3 \times 0.037 \times \exp^{[0.118 \times (\mathrm{Ts}-25)]}$ [*Skirrow*, 1975; *Wingate et al*., 2008]. Here we adopted a f_{CA} value of 20, which resulted in the best agreement between measured and modeled δ_R at this site during the experimental period [*Santos et al*., 2012].

The effective diffusivity of CO_2 in the soil air is given by

$$D_{18} = \alpha_d \left[D_{25} \theta_a^2 \left(\frac{\theta_a}{\theta_{\mathrm{sat}}} \right)^{\frac{3}{b}} \left(\frac{T_s + 273.16}{T_{25}} \right)^n \right] \tag{13}$$

where $\alpha_d = 1 + \varepsilon_d/1000$, where ε_d (−8.7‰) is the full kinetic fractionation in the soil pores, D_{25} is the molecular diffusivity of CO_2 (1.4×10^{-5} m^2 s^{-1}) at 298 K, θ_a is the proportion of soil pores filled with air, $\theta_a = \theta_{\mathrm{sat}} - \theta_w$, where θ_{sat} is the soil water content at saturation estimated to be 0.46 m^3 m^{-3} at the site [*Saxton and Willey*, 2006], b is the soil water retention parameter, determined to be 6.2 in this study [*Cosby et al*., 1984], $T_{25} = 298$ K, and n is 1.5 [*Bird et al*., 2002; *Stern et al*., 2001].

The isotope composition of CO_2 in isotopic equilibrium with the soil water [*Brenninkmeijer et al*., 1983] is given by

$$\delta_{\mathrm{eq},s} = \delta_{s,\mathrm{zeq}} + \frac{17,604}{(T_s + 273.16)} - 17.93 \tag{14}$$

where $\delta_{s,\mathrm{zeq}}$ is the isotopic composition of soil water at the equilibration depth (z_{eq}), $z_{\mathrm{eq}} = 2\sqrt{2 \ln 2 D_{18}/k_s B \theta_w}$, defined as the shallowest depth where full isotopic equilibration between water and CO_2 molecules occurs [*Wingate et al*., 2009]. The $H_2{}^{18}O$ composition of soil water (δ_s) determined from soil samples throughout

the experiment (section 3.2) was converted into the VPDB scale and used to estimate half-hourly δ_s. An interpolation procedure to estimate δ_s for times between samplings and exponential functions, adjusted using δ_s determined for three depths (section 3.2), was used to predict $\delta_{s,\mathrm{zeq}}$ [*Santos et al*., 2012; *Wingate et al*., 2008].

3. Experimental Methods

3.1. Site Description

The field experiment was conducted in a temperate deciduous forest at the Environment Canada research station in Borden, ON, Canada (44°19′N, 79°56′W) from mid-June to August 2009. The forest at this site is approximately 100 years old and represents natural regrowth on abandoned farm land. A survey in 2006 indicated the predominant tree species at the site were red maple (*Acer rubrum* L.), eastern white pine (*Pinus strobus* L.), large-tooth aspen (*Populus grandidentata* Michx.), and white ash (*Fraximus americana* L.), with percentages of occurrence of 52.2, 13.5, 7.7, and 7.1%, respectively [*Teklemariam et al*., 2009]. The stand height was approximately 22 m, and the leaf area index (±SE) ranged from 3.9 (±0.13) to 3.6 (±0.15) $m^2\ m^{-2}$ from June to September 2009. Textural analysis shows the soil at the site to be a loamy sand [*Santos et al*., 2012].

3.2. Isotope Measurements

Two tunable diode laser trace gas analyzers (TGA100, Campbell Scientific, Logan, UT, USA; hereafter TGA), one dedicated to CO_2 and the other to H_2O analysis, were used to measure the mixing ratios of $^{12}C^{16}O_2$, $C^{18}O^{16}O$, $H_2{}^{16}O$, and $H_2{}^{18}O$ above the forest. The δ_a was expressed according to the delta notation, in reference to Vienna Peedee Belemnite or VPDB scale, and δ_v was expressed in reference to the Vienna Standard Mean Ocean Water (VSMOW) standard [*Allison et al*., 1995; *Griffis et al*., 2005].

The air was drawn continuously from two air intakes, set up at 25.8 and 36.8 m above the ground, to the TGA sampling systems, kept in temperature-controlled enclosures set up in trailers. In this study, the measurements taken at 25.8 m were used for the estimates of δ_A (section 2.1). Typical differences of CO_2 concentration between the two air intakes above the canopy were quite small ($< 5\ \mu mol\ mol^{-1}$), so the use of concentration measurements obtained at 36.8 m would have negligible effect in δ_A calculations. To prevent condensation of water vapor in the sampling lines of the H_2O isotope TGA, the air inlet tubes were heated as described by *Lee et al*. [2007]. In the CO_2 isotopomer TGA, critical orifices located downstream of the heated air filters kept a low pressure in the sampling lines preventing condensation inside the tubing. Each intake was measured for 15 s during 4 min. At the end of each measurement cycle, gas was sampled from calibration tanks during 1 min. A detailed description of the calibration procedure of the CO_2 isotopomer TGA is provided by *Santos et al*. [2012]. Water and CO_2 isotope measurements were corrected for the nonlinearity of the TGAs using calibration gases as described in previous studies [*Bowling et al*., 2003; *Griffis et al*., 2005; *Lee et al*., 2007; *Welp et al*., 2008]. Simultaneous measurements of water and CO_2 isotopes were available from day of year (DOY) 187 to 232. Mixing ratios of water vapor and CO_2 isotopomers, used in this study, were measured during week days (Monday to Friday). Weekend measurements of CO_2 isotopomers were taken near the forest floor and have been reported by *Santos et al*. [2012], who also provided further details on experimental setup at the site.

The $H_2{}^{18}O$ compositions of bulk leaf (δ_{Lb}) and xylem (δ_x) water were determined for three tree species: red maple (*Acer rubrum* L.), large-tooth aspen (*Populus grandidentata* Michx.), and white ash (*Fraxinus americana* L.). Five to six red maple leaves and approximately 10 large-tooth aspen and white ash leaves were collected on each sampling day. The leaf samples had the center vein removed and were placed in sealed glass vials. Nongreen twigs from these species were also sampled, had the phloem removed, and were sealed in vials to determine δ_x. Leaf and twig samples were taken every 2–5 days at 12:00 EST during the experimental period excluding days when leaves were wet, for a total of 26 sampling times.

Soil samples were obtained near the flux tower at three depths: 5, 10, and 50 cm to determine the $H_2{}^{18}O$ composition of liquid water in the soil (δ_s). The soil samples were placed in sealed vials and kept refrigerated. The liquid water from soil samples was extracted using the cryogenic vacuum extraction method [*Ehleringer and Osmond*, 1989]. In addition, to determine the $H_2{}^{18}O$ composition of precipitation water (δ_p), rain water was also collected at the site on an event basis using a 15 cm diameter plastic funnel placed over a thermally insulated plastic bottle. Ground water samples were also collected from two wells at the site in two

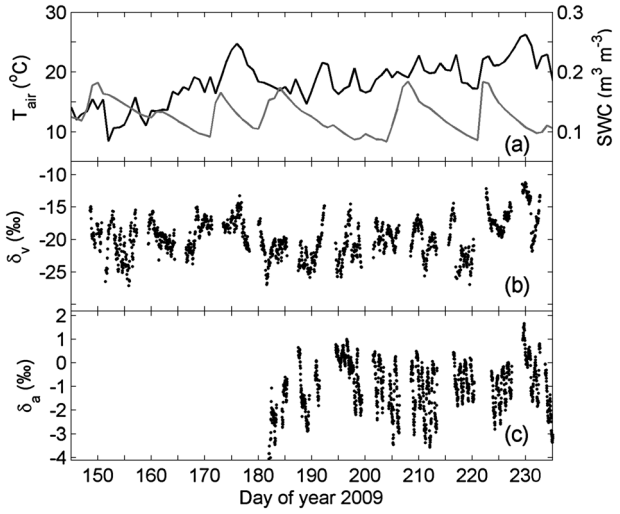

Figure 1. Time series of (a) daily average air temperature (T_{air}, black solid line) measured at 33 m and soil water content (SWC, gray solid line) obtained at 10 cm depth, (b) hourly values of $H_2{}^{18}O$ composition of water vapor in the air (δ_v), and (c) half-hourly values of $C^{18}OO$ composition of the air (δ_a). δ_a and δ_v are expressed in reference to the VPDB and VSMOW scales, respectively, in the delta notation, and were measured at 25.8 m above a temperate deciduous forest in Borden, ON, Canada.

dates during the growing season to determine $H_2{}^{18}O$ composition of ground water (δ_g). After each precipitation event, the rain water was transferred from the plastic bottle to a sealed glass vial. The δ_{Lb}, δ_x, δ_s δ_p, and δ_g of water samples were determined using the CO_2 equilibration method on a gas bench auto sampler attached to a mass spectrometer (Delta Plus XL, Thermo Finnigan, Bremen, Germany) with precision of 0.1‰. The $H_2{}^{18}O$ composition of liquid water was expressed relative to the VSMOW scale in the delta notation.

3.3. Supporting Measurements

The eddy covariance technique was used to measure F_N and latent heat flux above the forest. The three wind velocity components were measured using a sonic anemometer (SATI-Sx, ATI, Longmont, CO) set up at 33.4 m above the ground. A closed-path infrared gas analyzer (Li-6262, LI-COR, Lincoln, NE, USA) was used to determine the H_2O and CO_2 mixing ratios in the air at 33.4 m. The half-hourly eddy covariance CO_2 flux included in our analysis met the following criteria: direction ranging from 90° to 255° and friction velocity larger than 0.45 m s^{-1}, following *Teklemariam et al*. [2009] who also provide further details on the long-term eddy covariance measurements at the site. The eddy covariance data were used to optimize the physiological model described in Appendix A.

The soil CO_2 flux was measured using an automated dark chamber (LI-8100, LI-COR) with a diameter of 20 cm. The forest understory vegetation was sparse, and small seedlings growing inside the chamber collars were excluded. Chamber measurements were taken every 15 min and averaged into 30 min intervals. To correct single point measurements for the effects of spatial heterogeneity, the soil CO_2 flux was measured 2–3 times a week using the same gas analyzer and a portable chamber, at 30 locations near the flux tower. A linear regression model was then used to scale up the automated soil chamber measurements as described by *Santos et al*. [2012].

In addition, air temperature and relative humidity (HMP45A, Vaisala, Vantaa, Finland), photosynthetically active radiation (LI 190SB, LI-COR), and outgoing long-wave radiation (CNR1, Campbell Scientific) were measured at a height of 33.4 m. The precipitation was measured using a tipping bucked rain gauge (Belfort, Baltimore, MD) in a nearby open pond area. Soil temperature (T_s) and water content (θ_w) were measured using thermocouples (105T, Campbell Sci.) and soil moisture probes (CS615-L, Campbell Sci.), respectively, at a depth of 10 cm. Leaf wetness was monitored at 18 m and 10 m height using electronic flat plate sensors (237, Campbell Sci.), and these data were used to select times with no leaf wetness when interpreting model results.

4. Results and Discussion

4.1. Environmental Conditions and Isotope Compositions of CO_2 and Water Vapor in the Air

Daily average air temperature increased throughout the experiment, ranging from 8.4 (DOY 152) to 26.2°C on DOY 230 (Figure 1a). The total rainfall from June to August 2009 was 251 mm, which was above the long-term average of total precipitation (228 mm) measured in these months from 1989 to 2006 at a nearby weather station (Egbert, ON, Canada). The loamy sand texture leading to good soil drainage at the site

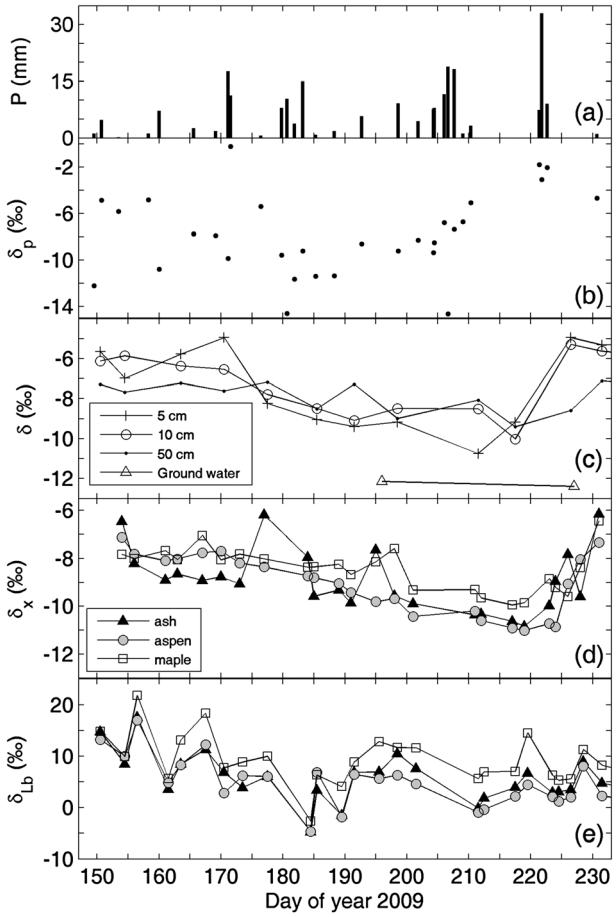

Figure 2. Time series of total precipitation during (a) rain events and $H_2{}^{18}O$ composition of (b) rain (δ_P), (c) soil water (δ_s) at three depths 5 cm, 10 cm, and 50cm ground water (δ_g), (d) xylem water (δ_x), and (e) observed leaf bulk water (δ_{Lb}) obtained from twig samples of white ash (*Fraxinus americana* L.), large-tooth aspen (*Populus grandidentata* Michx.), and red maple (*Acer rubrum* L.) in a temperate deciduous forest. The isotope composition of liquid water expressed relative to the VSMOW scale in the delta notation.

combined with frequent precipitation events (Figure 2a) was responsible for large variations in soil water content (Figure 1a), with values ranging from 0.08 (DOY 204) to 0.18 m^3m^{-3} (DOY 223).

Values of δ_a, measured above the forest canopy, showed a clear diurnal pattern for most days, with half-hour values reaching a maximum in the early evening (18:00 EST) and a minimum in the early morning (05:00 EST) (Figure 1b). The causes for the δ_a diurnal pattern are the expansion of the boundary layer during the day and entrainment of more enriched air from atmospheric layers above the surface as well as the retrodiffusion of CO_2 from the leaves to the air after isotopically equilibrating with foliage water [*Griffis et al*., 2005; *Yakir and Sternberg*, 2000].

Values of δ_v obtained above the forest showed large day-to-day variability, with hourly values varying from −27 to −11.2 ‰, and average δ_v equal to −19.7‰. *Welp et al*. [2012] used the oxygen and hydrogen isotope compositions of water vapor to study the mechanisms controlling the water vapor variability in the surface layer for six sites around the world, including our experimental period at the Borden forest. They postulated that evaporation from the Great Lakes during the summer months (June to August) added significant amounts of moisture to the surface layer at our study site.

4.2. Isotope Composition of Ecosystem Water Pools

The temporal variation of isotope composition of different ecosystem water pools, expressed in the VSMOW scale, is shown in Figure 2. Average δ_p, weighted by precipitation magnitude, was −7.7‰. However, large event-to-event variation in δ_p was observed during the experimental period, with values ranging from −14.6‰ (DOY 180 and 206) to −0.2 ‰ on DOY 171 (Figure 2b). Event-to-event variations in δ_p are related to differences in the trajectory and in the isotope composition of water sources of different storm systems [*Welker*, 2000]. At the Borden forest, the Great lakes are expected to be a significant source of moisture for precipitation during the summer [*Bowen and Revenaugh*, 2003].

Figures 2c and 2d show δ_s and δ_x variation during the growing season. Values of δ_s and δ_x showed a downward trend from the beginning of the measurements until approximately DOY 220 when values of these variables started to increase following large rainfalls on DOY 221 and 222, in which total precipitation was 49.4 mm and δ_p was more enriched than in the previous precipitation events. Large δ_s vertical gradients were not observed at this site (Figure 2c) in comparison to previous studies [*Seibt et al*., 2006]. The largest difference between δ_s values at 5 and 50 cm (3.6‰) was observed after precipitation events on DOY 221 and 222. Average δ_g was −12.3‰, and small variation in δ_g (0.3‰) was observed between sampling dates (Figure 2c).

Table 1. Coefficient of Determination (R^2), Root Mean Square Deviation (RMSD), and Mean Error (ME) for the Relationships Between Midday Measured (δ_{Lb}) and Modeled Isotope Compositions of Leaf Water (Using the CG [*Craig and Gordon*, 1965] and FC [*Farquhar and Cernusak*, 2005] Models (Equations (4) and (7) With Measured Isotope Composition of Xylem Water) for White Ash (*Fraxinus americana* L.), Large-Tooth Aspen (*Populus grandidentata* Michx.) and Red Maple (*Acer rubrum* L.)

	CG Model			FC Model		
Tree	R^2	RMSD (‰)	ME (‰)	R^2	RMSD (‰)	ME (‰)
Ash	0.88	3.6	3.3	0.75	2.1	−0.10
Aspen	0.75	4.6	4.1	0.78	2.0	−0.14
Maple	0.85	1.8	−0.4	0.78	2.0	0.04
Average	0.88	2.7	2.3	0.75	2.1	−0.10

The row labeled "Average" shows comparison of measured isotope composition of bulk leaf water averaged for the three species and modeled values obtained using the average isotope composition of xylem water in equations (4) and (7). The effective diffusion length (L) needed for the FC model was optimized for each species and for the average conditions.

Average δ_x values were −9.1, −8.9, and −8.4‰ for large-tooth aspen, white ash, and red maple, respectively (Figure 2d). The mean δ_x values were more negative than average values of δ_s: −7.3, −7.3, and −7.9‰ at 5, 10, and 50 cm, respectively. This may be an indication that all species utilized water from deeper layers in the soil, close to the water table, which had water more depleted in $H_2{}^{18}O$ (Figure 2c). A large spike in δ_x of ash (DOY 177) was observed after a precipitation event on DOY 171, in which δ_p was more enriched (0.2‰) than in previous rainfalls. This spike in δ_x indicates that the ash tree probably has a shallower rooting depth distribution than the other two species, which allows capturing short duration precipitation events with often more enriched precipitation water, while having also the ability to extract water from deeper soil layers, which was indicated by more negative values of δ_x than the values of δ_s observed at the soil surface. Values of δ_{Lb} measured at midday showed a large day-to-day variability, ranging from −4.8 to 17.6‰ for large-tooth ash, −4.7 to 17.0‰ for aspen, and −2.7 to 21.8‰ for red maple. This variation is related to other variables besides δ_x and will be discussed in the next section.

4.3. Calculated Isotope Composition of Leaf Water

Comparisons between measured and modeled δ_{Lb}, using δ_x of white ash, large-tooth aspen, and red maple, showed R^2 ranging from 0.75 to 0.88 (CG) and 0.75 to 0.78 (FC) (Table 1). The RMSD for this comparison ranged from 1.8 to 4.6‰ (CG) and 2.0 to 2.1‰ (FC). Estimates provided by the FC model are sensitive to the effective diffusion length (L) of the Péclet effect (equation (9)), which is a poorly constrained parameter in leaf isotope enrichment models and has been assumed to be species-specific [*Ferrio et al*., 2009; *Song et al*., 2013; *Xiao et al*., 2012]. In this study, we optimized L values to improve the agreement between δ_{Lb} measurements and the predicted values obtained by the FC model using equation (7). The optimized L values ranged from 0.1 mm (ash and aspen) to 0.2 mm (maple). Our results suggest that the Péclet effect on $H_2{}^{18}O$ leaf enrichment is negligible at the canopy scale, which has also been reported in recent studies [*Xiao et al*., 2012; *Xiao et al*., 2010]. A negligible P implies that the foliage water pool is well mixed; however, previous studies show L does not scale up well from the leaf to the canopy scale and further investigation on the behavior of L in canopy-scale leaf water isotope composition models is needed [*Griffis*, 2013].

Lee et al. [2009] demonstrated that turbulent mixing enhances the isotope kinetic fractionation at the canopy scale. The inclusion of aerodynamic resistance in the kinetic fractionation calculations improved the agreement between modeled and measured δ_{Lb} in agricultural ecosystems [*Griffis et al*., 2011; *Xiao et al*., 2012]. Here, we evaluated the sensitivity of δ_{Lb} estimates to turbulent effects by excluding r_a from $\varepsilon_{k,w}$ calculations (equation (5)). The exclusion of r_a resulted in small differences in model accuracy (RMSD variation < 1.2‰) for both CG and FC models (Table 1). The effect of turbulence on canopy-scale kinetic fractionation will be discussed further in the next section.

Figure 3 shows the comparison between observed midday δ_{Lb} and predicted values using the CG and FC models. The CG model overestimated δ_{Lb} indicating that a departure from steady state conditions occurred at our site at midday. Although, we could not evaluate the FC and CG model performance throughout the entire day because leaf water was sampled only at midday, our results indicate that nonsteady state

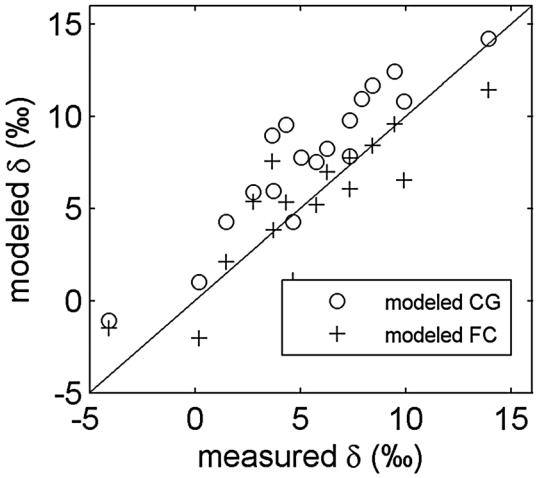

Figure 3. Comparison between modeled values of $H_2{}^{18}O$ composition of leaf water (VSMOW) assuming steady state ($\delta_{Lb,s}$ equation (4), CG model) and nonsteady state (δ_{Lb} equation (7), FC model) and average values obtained at midday from leaf samples of white ash (*Fraxinus americana* L.), large-tooth aspen (*Populus grandidentata* Michx.), and red maple (*Acer rubrum* L.) in a temperate deciduous forest.

effects are strong at the site. A larger departure from steady state is expected to occur at night (supplemental material) and has been confirmed in intensive sampling field campaigns of δ_{Lb} [*Welp et al*., 2008; *Xiao et al*., 2012] and high temporal resolution (30 min) δ_{Lb} data derived from branch chamber measurements [*Wingate et al*., 2010]. However, our results show a departure from steady state conditions even at midday conditions. The implications of nonsteady state conditions on δ_A calculation will be further explored in the next section.

4.4. Temporal Dynamics of Isotope Composition of Ecosystem CO_2 Fluxes

Figure 4 shows half-hourly values of isotope composition of net CO_2 assimilation and some of the variables used for its estimation during a selected week. A noteworthy feature in this graph is the coupling between δ_a and $H_2{}^{18}O$ composition of leaf water at the evaporative site (Figures 4a and 4b). During this selected period, the daytime correlation coefficients for the relationship between δ_a and $\delta_{Le,s}$ (CG model, equation (4)) were $r = 0.83$ ($p < 0.0001$) and $r = 0.72$ ($p < 0.0001$) for the nighttime. However, when nonsteady state effects were considered, higher correlation coefficients were observed for δ_a and δ_{Le} (FC model, equation (6)), with $r = 0.90$ ($p < 0.0001$) during the daytime and $r = 0.63$ ($p < 0.0001$) for nighttime. The coupling between δ_a and modeled δ_{Le} is an indication of the influence of the canopy on δ_a dynamics above the forest. The higher correlations between δ_a and δ_{Le} during the daytime are related to the larger exchange of CO_2 between the vegetation, when canopy resistance was lower and the turbulent mixing was more intense.

The canopy CO_2 retroflux represented by the ratio $C_c/(C_c - C_a)$, estimated using a physiological model (Appendix A), showed a distinct diel cycle (Figure 4c), with more negative values during the nighttime, when the difference between C_c and C_a was smaller than during the day. The daytime $r_{c,w}$ estimates, provided by the physiological model, were in agreement with $r_{c,w}$ derived from the Penman-Monteith equation and eddy covariance measurements (Figure A1). In the nighttime, however, the physiological model $r_{c,w}$ estimates were higher than calculated using the Penman-Monteith equation, so we assumed a constant nighttime canopy resistance equal to the average $r_{c,w}$ derived from the Penman-Monteith equation (further details in Appendix A). Values of $r_{c,w}$ were about 1 order of magnitude larger than r_a and $r_{b,w}$ (Figure 4d). Daytime average r_a, $r_{b,w}$, and $r_{c,w}$ were 18, 12, and 250 s m^{-1}, respectively, while during the nighttime, average values for those resistances were 70, 13, and 1000 s m^{-1}, respectively (Figure 4d). The average $\varepsilon_{k,c}$ during the selected period was 8.3‰; however, $\varepsilon_{k,c}$ variation was up to 0.8‰ between sequential half-hour periods (Figure 4e). When turbulence effects were not considered in $\varepsilon_{k,c}$ calculations, average $\varepsilon_{k,c}$ was slightly larger (8.7‰). The influence of the aerodynamic resistance on $\varepsilon_{k,c}$ was limited in our study because of the small magnitude of the ratio between r_a and r_c. Over rough surfaces, such as forest canopies, the aerodynamic resistance is small and plays a minor role in the exchange of mass and energy relative to its influence on short vegetation surface-atmosphere exchange. Differences in turbulent mixing and transpiration rates between tall and short plant canopies can have a significant impact on the variables governing the isotopic exchange. *Still et al*. [2009] used a land surface model to study the isotopic exchange in a broad leave deciduous forest in a C4 grassland. Their results show that the relative humidity within the grass canopy was higher than the one determined for forest ecosystem, due to higher transpiration rates in grasslands. Higher relative humidity values resulted in more depleted leaf water isotopic composition in the grassland in comparison to that of the forest canopy, even when all the other forcing variables in their model were kept constant. So, turbulence

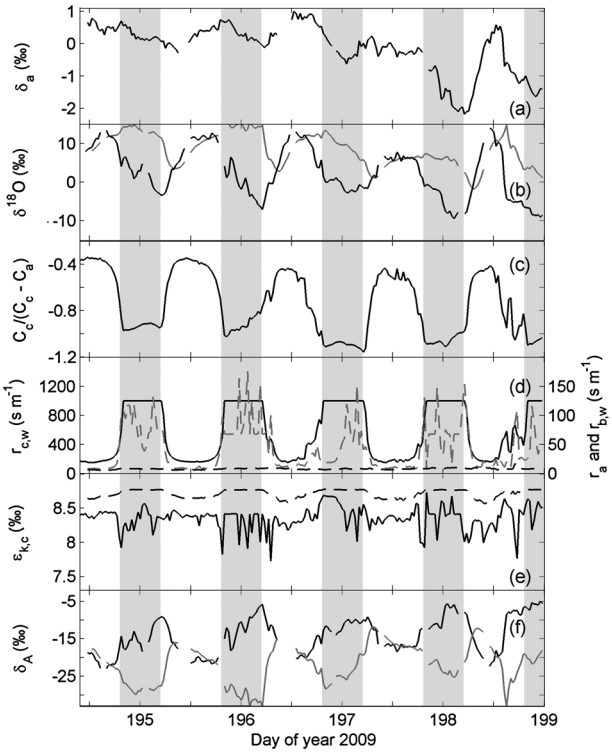

Figure 4. Half-hourly values of (a) $C^{18}OO$ composition of the air (δ_a) at 25.8 m; (b) $H_2{}^{18}O$ composition of leaf water at the evaporating site (VSMOW scale) assuming steady state ($\delta_{Le,s}$ black solid line, equation (4)) and nonsteady state (δ_{Le}, gray solid line, equation (6)) conditions; (c) CO_2 retroflux of CO_2, represented by the fraction $C_c/(C_c - C_a)$; (d) resistances values of canopy (r_c, solid black line), boundary layer (r_b, dashed black line) and aerodynamic (r_a, dashed blue line) to H_2O diffusion; (e) CO_2 canopy-scale kinetic fractionation factor ($\varepsilon_{k,c}$), calculated considering (black solid line) and ignoring (dashed line) turbulence effects, and (f) $C^{18}OO$ composition of the canopy CO_2 flux (δ_A), calculated using δ_{Le} assuming steady state (black line) and nonsteady state (gray line) conditions. The shaded areas in the graph indicate night time periods.

effects can have a great impact on gas exchange in plant canopies and should always be considered in ecosystems scale studies.

Half-hourly values of δ_A, calculated using equation (2) and values of δ_{Le}, derived from the CG (equation (4)) and FC (equation (6)) models, are shown in Figure 4f. Differences between nighttime values of δ_A, calculated assuming steady state and nonsteady state conditions, were large (up to 27‰). During the daytime, the average difference between δ_A values calculated assuming steady state and nonsteady state conditions was 3.5‰. Although these daytime differences in δ_A values are much smaller than the differences in δ_A values obtained at the nighttime, these differences can be significant for CO_2 flux partitioning, considering that canopy CO_2 fluxes are large during the daytime and the typical values of *Deq* found for this site (data shown below).

Average modeled daytime δ_A was obtained from half-hourly δ_A, calculated using FC model δ_{Le} estimates, and excluding half-hour periods when the leaf wetness duration sensors indicated the presence of liquid water, and periods of inadequate fetch (Figure 5a). Average daytime δ_R was calculated using half-hourly δ_R estimated using equation (11). Daytime average values of modeled δ_R are shown in Figure 5a. The daytime average δ_R reached its minimum value (−24.6‰) on DOY 210 and then increased steadily until DOY 225 when average δ_R was −9.6‰. The temporal dynamics of δ_R were driven mainly by δ_s (Figure 2b). Precipitation events on DOY 221 and 222 resulted in significant enrichment of δ_s and consequently δ_R. Evaporative enrichment of δ_s can produce large vertical gradients of δ_s near the soil surface [*Dubbert et al*., 2013]. Due to budget constraints, we only measured δ_s at three soil depths, but future studies should consider a sampling scheme that include more depths specially close to the surface where δ_s variation is expected to be large.

The range of modeled δ_R values obtained in this study are in agreement with observations reported by *Santos et al*. [2012] who observed half-hourly measured δ_R ranging from −31.4‰ to −11.2‰ for four selected periods during the growing season in this same ecosystem. These modeled δ_R are similar with the δ_R obtained using soil chamber for a corn ecosystem in Minnesota [*Griffis et al*., 2011] and at a southern boreal forest ecosystem in Canada [*Flanagan et al*., 1997] but much lower than δ_R values reported by *Seibt et al*. [2006] for a forest ecosystem in the UK and by *Wingate et al*. [2008] in a Mediterranean ecosystem in southern Portugal.

Average daytime δ_A showed large day-to-day variation throughout the experiment (Figure 5), with values ranging from −19.1 (DOY 195) to −11.3‰ on DOY 205. The average daytime δ_A for the whole period was −16.2‰. This average δ_A was used to calculate the $C^{18}OO$ canopy-scale discrimination factor (Δ), assuming $\Delta \approx \delta_a - \delta_A$ [*Lee et al*., 2009], which ranged from 10.5 (DOY 189) to 20.8‰ (DOY 195). *Wingate et al*. [2010] reported a $C^{18}OO$ discrimination factor, obtained from branch chamber measurements, ranging

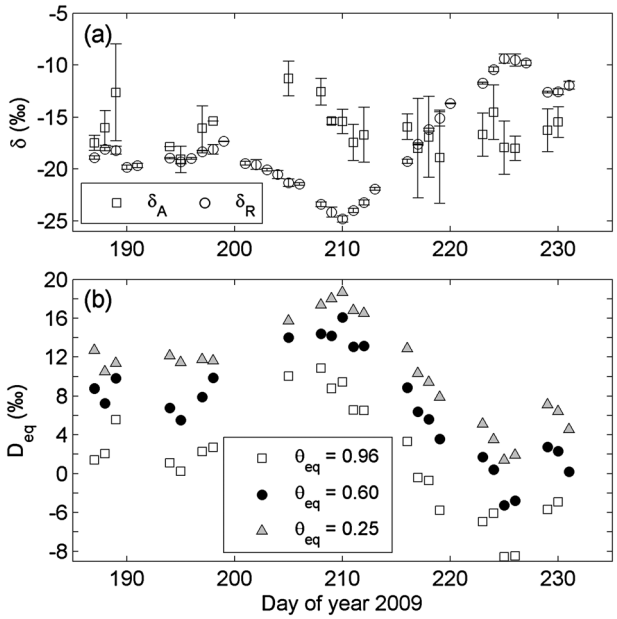

Figure 5. (a) Daytime average (± 1 standard deviation) $C^{18}OO$ composition of canopy net CO_2 flux (δ_A) and net soil CO_2 flux (δ_R); (b) and absolute daytime values of isotope disequilibrium, $D_{eq} = \delta_R - \delta_A$, in a temperate deciduous forest from July to August 2009. In Figure 5b, δ_A was calculated assuming different values for the extent of the CO_2 hydration in the leaves (θ_{eq}).

mostly from 10 to 25‰ in a Maritime pine stand during the growing season. The values of Δ obtained in this study are in agreement with the canopy-scale discrimination factor values calculated by *Griffis et al.* [2011] for a corn canopy. They observed a decrease of the canopy evaporative isotope enrichment caused by a higher relative humidity and also reported lower δ_{Lb} in their ecosystem during rain events. In our study, higher relative humidity also reduced δ_{Lb} and δ_{Le} values (data not shown).

We evaluated the effect of lower values of $\theta_{eq.}$ on the $C^{18}OO$ disequilibrium (D_{eq}) seasonal dynamics in this ecosystem. Daytime average δ_R and δ_A, modeled using equation (2) and three values of θ_{eq}, were used to calculate D_{eq}, excluding half-hour periods when leaf wetness sensors indicated the presence of liquid water over the canopy or when wind direction did not provide adequate fetch for the site. Values of D_{eq} showed a large temporal dynamics throughout the season, with highest values observed near DOY 210, when the lowest δ_R values were estimated for the experimental site (Figure 5b). The magnitude of D_{eq} was strongly influenced by the value of θ_{eq}. Average absolute values of D_{eq} for the whole period were 4.8, 7.4, and 10.6‰ for θ_{eq} values of 0.96, 0.60, and 0.25, respectively. A strong D_{eq} was observed on DOY 210, when the isotope disequilibrium at the site reached 18.7, 16.1, and 9.4‰ assuming θ_{eq} equal to 0.25, 0.6, and 0.96, respectively. Throughout the season, the magnitude of D_{eq} was indirectly proportional to θ_{eq}, except toward the end of the growing season, on DOY 225 and 226, when highest absolute D_{eq} values (8.5‰) were obtained for $\theta_{eq} = 0.96$.

The inverse relationship between θ_{eq} and D_{eq} was not expected, based on previous studies The expected relationship is that higher hydration efficiencies in the canopy, i.e., higher θ_{eq}, result in higher rates of oxygen atom exchange between CO_2 and enriched water molecules in the foliage. When these CO_2 molecules diffuse back to the atmosphere, the difference between δ_A and δ_R is expected to increase, resulting in higher magnitude in D_{eq}. However, depleted ^{18}O precipitation at our site throughout the growing season (Figure 2b) resulted in quite negative δ_R values, which were often lower than δ_A (Figure 5a). Under this condition ($\delta_A > \delta_R$), the increase of hydration efficiency would result in more negative values of δ_A (equation (2)), so δ_A would approach δ_R therefore producing lower D_{eq} as θ_{eq} approaches 1. The expected relationship between θ_{eq} and D_{eq} was observed after DOY 219, when precipitation events with more enriched δ_p resulted in more positive δ_R (Figure 5b). Consequently, increased θ_{eq} lead to more negative δ_A and resulted in a larger absolute D_{eq}. This inverse relationship between θ_{eq} and D_{eq} is expected to occur in mid latitude ecosystems, where δ_R is expected to be much larger than the values observed in this study [*Wingate et al.*, 2008].

Previous studies have shown a relationship between the magnitude of D_{eq} and precipitation events. *Sturm et al.* [2012] observed a reduction in δ_A caused by precipitation in a mixed deciduous forest. They attributed this decrease in δ_A to lower canopy evaporative isotope enrichment due to higher relative humidity during rainy days. *Griffis et al.* [2011] observed a seasonal variation in $C^{18}OO$ disequilibrium in a corn canopy and low D_{eq} during rainy periods. *Wingate et al.* [2010] also reported a reduction in D_{eq} during rain events, because the precipitation water reset the ecosystem water pools to the same isotopic composition as δ_p. However, our results show that precipitation events during the growing season caused an increase of D_{eq} at

the Borden Forest. The magnitude of D_{eq} was closely related to δ_p, which was the main variable affecting δ_s (Figures 2b and 2c). Low values of δ_s near the soil surface (5 cm depth) on DOY 210 were responsible for a significant reduction in δ_R (Figure 5b), which led to a strong D_{eq} over the same period (Figure 5b). These results point to a need for ecosystem specific assessments of D_{eq} and consideration of the temporal dynamics of D_{eq}.

The strong predicted D_{eq} indicates that $C^{18}OO$ has a great potential to be used as tracer to study carbon exchange in natural ecosystems. However, the large temporal variability of δ_p at our site shows that an event-based precipitation sampling strategy is required to interpret the temporal dynamics of soil and plant isotope signals in this ecosystem. In addition, to improve the accuracy in D_{eq} estimates, a better understanding of the mechanisms controlling the extent of canopy CO_2 hydration is needed. Our results show that D_{eq} is highly sensitive to θ_{eq} (equation (2)), emphasizing the need for canopy-scale studies to investigate the extent of CO_2 hydration at the ecosystem scale and appropriate schemes to scale up variables derived from leaf observations to canopy-scale isotope models.

5. Conclusions

Bulk leaf water isotope composition showed large day-to-day variability at our research site with values ranging from −2.7 to 21.8‰. Leaf water enrichment simulations indicate that nonsteady state effects were important even at midday in your site and should be considered when estimating δ_A. The inclusion of turbulence effects resulted in small improvement of δ_{Lb} estimates in this study, which is related to the small magnitude of the aerodynamic resistance compared to the relatively large canopy resistance in the forest.

Values of δ_A showed large day-to-day variation at our site, with daytime average values ranging from −19.1 to −11.3‰. The dynamics of δ_R were mainly driven by precipitation events with variable δ_p. Large D_{eq} values (up to 11‰ for $\theta_{eq} = 0.96$) were observed at our site; however, the magnitude of the disequilibrium was variable throughout the season, and near zero D_{eq} values were observed near the end of the experimental season for $\theta_{eq} = 0.96$. The temporal dynamics of D_{eq} was largely driven by the variability of δ_p at the site, which was demonstrated by our high-frequency sampling scheme for precipitation water. The magnitude of D_{eq} was also very sensitive to the hydration efficiencies in the canopy. For this temperate forest during most of the growing season, the magnitude of D_{eq} was inversely proportional to θ_{eq}, due to the very negative δ_R signal, which is contrary to observations for other ecosystems investigated in previous studies. The large D_{eq} values observed at our site indicate that $C^{18}OO$ can be a very powerful tool for partitioning plant and soil components of the net CO_2 ecosystem exchange. However, additional work is still needed to understand better the mechanisms controlling the extent of CO_2 hydration in foliage and soils.

Appendix A

A plant physiological model was used to estimate some physiological variables, such as $r_{c,c}$ and C_c used to calculate δ_A and $\delta_{L,e}$ (section 2.1). In this approach, the canopy-scale stomatal resistance is derived from the net CO_2 assimilation, which is a function of environmental variables such as water vapor deficit, photosynthetically active radiation, and canopy temperature [*Calvet et al.*, 2004]. The leaf-scale conductance for CO_2 ($g_{l,c}$) is expressed as

$$g_{l,c} = \frac{g_{\min}}{1.6} + \frac{\left\{ A_n - A_{\min}\left(\frac{D_s}{D_{\max}}\right)\left[\frac{(A_n+R_d)}{(A_m+R_d)}\right] + R_d\left[1 - \frac{(A_n+R_d)}{(A_m+R_d)}\right]\right\}}{C_a - C_i} \tag{A1}$$

where $g_{\min}$ is the cuticular conductance for water vapor—in this study we adopted the $g_{\min}$ value (0.15 mm s^{-1}) found by *Calvet et al.* [2004] for woody broadleaved species—A_n is the leaf net assimilation, A_m is photosynthetic rate at saturating light intensity, $A_{\min}$ is the residual photosynthesis rate, D_s is leaf-to-air saturation deficit (g kg^{-1}), $D_{\max}$ is the maximum D_s in well-watered conditions, R_d is the dark respiration, and $R_d = 0.11A_m$, where A_m is given by

$$A_m = A_{m,\max}\left\{1 - \exp\left[\frac{-g_m(C_i - \Gamma)}{A_{m,\max}}\right]\right\} \tag{A2}$$

where g_m is the unstressed mesophyll conductance and Γ is the CO_2 compensation point. The variables

g_m, Γ, and $A_{m,\max}$ are functions of the canopy temperature and were estimated using Q_{10}-type functions as described by *Jacobs* [1994]. The leaf internal CO_2 concentration was estimated using the following closure equation:

$$C_i = fC_a + (1-f)\Gamma \tag{A3}$$

where f is the coupling factor given by

$$f = f_0\left(\frac{1-D_s}{D_{\max}}\right) + \left(\frac{g_{\min}}{g_{\min}+g_m}\right)\left(\frac{D_s}{D_{\max}}\right) \tag{A4}$$

where f_0 is the maximum ratio of the intercellular to the atmospheric CO_2 concentration, when D_s is zero, $f = f_0$.

The net assimilation is limited by photosynthetically active radiation (*PAR*) and is calculated as

$$A_n = (A_m + R_d)\left\{1 - \exp\left[\frac{-\varepsilon PAR}{A_m + R_d}\right]\right\} - R_d \tag{A5}$$

where ε is the light conversion efficiency, $\varepsilon = \varepsilon_0(C_i - \Gamma)/(C_i - 2\Gamma)$, where $\varepsilon_0 = 0.017$ mg CO_2 J^{-1}.

The residual photosynthesis rate is expressed as

$$A_{\min} = g_m g_{\min}\frac{C_a - \Gamma}{g_m + g_{\min}} \tag{A6}$$

The parameters f_o and $D_{\max}$ were tuned [*Calvet et al*., 2004; *Xiao et al*., 2010] to improve the agreement between measured and simulated values of canopy CO_2 flux. Measured canopy CO_2 flux was assumed to be the difference between the net CO_2 ecosystem exchange and soil CO_2 flux, obtained using the eddy covariance technique and soil chamber measurements, respectively. The canopy CO_2 flux was estimated as follows:

$$F_A = \frac{C_i - C_a}{r_a + r_{b,c} + r_{c,c}} \tag{A7}$$

The aerodynamic resistance (r_a) was estimated based on the logarithmic wind profile:

$$r_a = \frac{\ln(z_m/z_0)}{k^2\overline{u}}\Phi_M \tag{A8}$$

where z_m is the measurement height, z_0 is the roughness length, k is the von Karman constant ($k = 0.4$), u is the wind speed at the measurement height, and Φ_M is the dimensionless stability function.

The boundary layer resistance ($r_{b,c}$) is given by

$$r_{b,c} = 1.4 \times \frac{b_r}{2LAI} \times \left(\frac{l_w}{u}\right) \tag{A9}$$

where $b_r = 283$ $s^{0.5}$ m^{-1}, l_w is leaf dimension, and *LAI* is the leaf are index.

The canopy resistance ($r_{c,c}$) was estimated from scaling up $g_{l,c}$ [*Ronda et al*., 2001], which integrates A_n and R_d over the canopy, assuming an exponential decay of *PAR* within the canopy as follows:

$$\frac{1}{r_{c,c}} = \int_0^{LAI}\left[\frac{g_{\min,w}}{1.6} + \frac{a(A_n + R_d)}{(C_s - \Gamma)\left(1 + \frac{D_s}{D_*}\right)}\right]dL \tag{A10}$$

where a is equal to $1/(1-f_0)$, D_* is $D_0/(a-1)$ and L is the leaf area. An analytical solution for equation (A10) is provided by *Ronda et al*. [2001].

The CO_2 concentration in the chloroplasts of the leaves (C_c), used to estimate the isotope composition of the canopy CO_2 flux (equation (2)), was calculated according to *Xiao et al*. [2010] as follows:

$$C_c = C_a + F_c\left(r_a + r_{b,c} + r_{c,c} + r_m\right) \tag{A11}$$

where r_m is the canopy-scale mesophyll resistance, given by $r_m = 1/(g_m LAI)$. Average daytime (10:00–15:00 EST) values of C_a, C_i, and C_c during the experiment were 378.4, 202.2, and 126.3 μmol mol^{-1}.

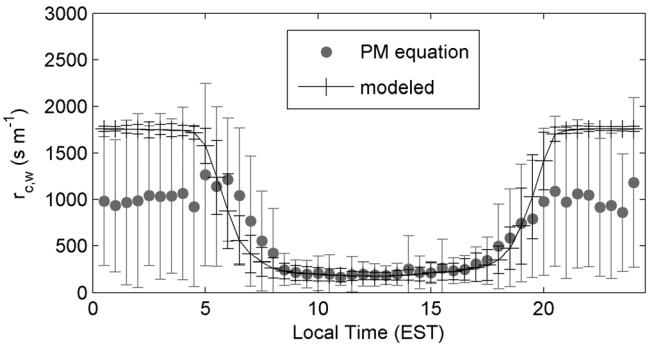

Figure A1. Ensemble average half-hourly values of canopy resistance to water vapor ($r_{c,w}$, ± 1 standard deviation) modeled using a physiological model and derived from the Penman-Monteith (PM) equation.

Typical differences between C_i and C_c are within the range of values reported in the literature [*Flexas et al.*, 2008; *Keenan et al.*, 2010].

Optimized values of f_o and D_o found for this study were 0.55 and 33 g kg^{-1}, respectively, which are within the range of values reported for broad leaved woody species [*Calvet et al.*, 2004]. Comparisons between F_c derived from flux measurements and estimated using the big-leaf model showed $R^2 = 0.85$ and root mean square error of 3.4 μmol m^{-2} s^{-1}. The inclusion of the soil water stress corrections proposed by *Calvet et al.* [2004] in the plant physiological model calculations did not improve F_c estimates, which indicates that the vegetation at the site was not under water stress.

To evaluate the performance of this physiological approach, the canopy resistance was compared to estimates obtained from the Pennan-Monteith (PM) equation and eddy covariance measurements as follows:

$$r_{c,w} = \frac{D}{\overline{w'\rho'_w}} + r_t\left(\frac{\overline{w'T'}}{\overline{w'\rho'_w}}s - 1\right) \tag{A12}$$

where $r_{c,w}$ is the canopy resistance to H_2O diffusion, given by $r_{c,w} = r_{c,c}/1.6$, D is the vapor density deficit, $\overline{w'\rho'}$ is the water vapor flux, $\overline{w'T'}$ is the sensible heat flux, s is the slope of the saturation vapor density curve, and r_t is total resistance ($r_t = r_a + r_{b,w}$), where $r_{b,w}$ is the boundary layer resistance to water vapor diffusion given by $r_{b,w} = r_{b,c}/1.4$. For the calculation of $r_{c,w}$ using equation (A12), we exclude periods, in which the wind speed did not satisfy the fetch conditions for the site, periods with $u^* < 0.45$ m/s, and when leaf wetness sensors indicate the presence of water in the forest canopy.

Figure A1 shows the comparisons between half-hour daily ensemble average of $r_{c,w}$ calculated using the physiological model and the PM equation. During the daytime, reasonable agreement was obtained by the two methods, indicating that the physiological model used at this study was suitable to estimate daytime $r_{c,w}$. However, at nighttime the physiological model overestimated $r_{c,w}$, when compared to half-hour $r_{c,w}$ values estimated using PM equation. This could be related to limitations of the approach used to scale up leaf resistance to the canopy scale. To overcome this problem, we adopted a constant value of resistance at nighttime equal to the average $r_{c,w}$ (1001 s m^{-1}) calculated using the PM equation during dew and rain free nights.

List of Symbols

A_m	photosynthetic rate at saturating light intensity, mg CO_2 m^{-2} s^{-1}.
$A_{m,\max}$	maximum photosynthetic rate at saturating light intensity, mg CO_2 m^{-2} s^{-1}.
$A_{\min}$	residual photosynthesis rate, mg CO_2 m^{-2} s^{-1}.
A_n	the leaf net assimilation, mg CO_2 m^{-2} s^{-1}.
B	Bunsen solubility coefficient for CO_2, m^3 of air m^{-3} of water.
B	slope of the soil water retention function.
C	density of liquid water, mol m^{-3}.
C_a	CO_2 molar concentration in the air, μmol m^{-3}.
C_c	CO_2 molar concentration in the chloroplasts, μmol m^{-3}.
C_i	CO_2 molar concentration in the intercellular space, μmol m^{-3}.
D	diffusivity of $H_2{}^{18}O$ in water, m^2 s^{-1}.
D_{18}	effective diffusivity of $C^{18}OO$ in the soil air, m^2 s^{-1}.
D_{25}	the molecular diffusivity of CO_2 at 298 K, m^2 s^{-1}.
D_{eq}	$C^{18}OO$ disequilibrium, ‰ VPDB.

D_{max}	maximum leaf-to-air saturation deficit, g kg^{-1}.
D_s	leaf-to-air saturation deficit, g kg^{-1}.
E_T	transpiration rate of the foliage, mol m^{-2} s^{-1}.
F	intercellular and atmospheric CO_2 concentration factor.
f_0	maximum ratio of the intercellular to the atmospheric CO_2 concentration.
F_A	canopy CO_2 flux, μmol m^{-2} s^{-1}.
f_{CA}	relative increase in CO_2 hydration resulting from the carbon anhydrase enzyme activity in the soil.
F_N	Net CO_2 ecosystem exchange, μmol m^{-2} s^{-1}.
F_R	soil CO_2 flux, μmol m^{-2} s^{-1}.
$g_{c,c}$	canopy-scale conductance to CO_2, m s^{-1}.
$g_{l,c}$	leaf-scale conductance to CO_2, m s^{-1}.
g_m	unstressed mesophyll conductance, m s^{-1}.
g_{min}	cuticular conductance to water vapor, m s^{-1}.
h	relative humidity.
k	von Karman constant.
k_h	rate of oxygen isotope exchange between CO_2 and water, s^{-1}
k_s	effective rate of oxygen exchange between CO_2 and liquid water, s^{-1}.
L	effective diffusion length, m.
LAI	he leaf are index, m^2 m^{-2}.
l_w	leaf dimension, m.
M_w	water molar mass, kg mol^{-1}.
P	Péclet number.
PAR	photosynthetically active radiation, J m^{-2} s^{-1}.
$q(T_c)$	saturation specific humidity at the canopy surface, kg m^{-3}.
q_a	specific humidity at the reference height, kg m^{-3}.
r_a	aerodynamic resistance, s m^{-1}.
$r_{b,c}$	boundary layer resistance to CO_2, s m^{-1}.
$r_{b,w}$	boundary layer resistance to H_2O, s m^{-1}.
$r_{c,c}$	canopy resistance to CO_2, s m^{-1}.
$r_{c,w}$	canopy resistance to H_2O, s m^{-1}.
R_d	dark respiration, mg CO_2 m^{-2} s^{-1}.
U	wind speed, m s^{-1}.
u^*	friction velocity, m s^{-1}.
v_{inv}	invasion velocity, m s^{-1}.
W	foliage water content, mol m^{-2}.
w_i	mole fraction of (light) water in the intercellular space, mol mol^{-1}.
z_{eq}	equilibration depth, m.
z_m	measurement height, m.
z_0	roughness length, m.
α_k	fractionation factor.
δ_A	$C^{18}OO$ composition of canopy of CO_2 flux, ‰ VPDB.
δ_a	$C^{18}OO$ composition of the air, ‰ VPDB.
$\delta_{eq,s}$	isotopic composition of CO_2 in isotopic equilibrium with the soil water, ‰ VPDB.
δ_g	$H_2{}^{18}O$ composition of ground water, ‰ VSMOW.
δ_{Lb}	$H_2{}^{18}O$ composition of leaf bulk water, ‰ VSMOW.
$\delta_{Lb,s}$	$H_2{}^{18}O$ composition of leaf bulk water assuming steady state conditions, ‰ VSMOW.
$\delta^P_{Lb,s}$	$H_2{}^{18}O$ composition of leaf bulk water assuming steady state conditions, calculated taking into consideration the Peclet effect, ‰ VSMOW.
δ_{Le}	$H_2{}^{18}O$ composition of leaf water at the evaporation sites, ‰ VSMOW.
$\delta_{Le,s}$	$H_2{}^{18}O$ composition of leaf water at the evaporation sites assuming steady state conditions, ‰ VSMOW.
δ_R	$C^{18}OO$ composition of soil CO_2 flux, ‰ VPDB.
δ_s	$H_2{}^{18}O$ composition of soil water, ‰ VSMOW.
$\delta_{s,zeq}$	$H_2{}^{18}O$ composition of soil water at the equilibration depth, ‰ VSMOW.

δ_v	$H_2{}^{18}O$ composition of water vapor, ‰ VSMOW.
δ_x	$H_2{}^{18}O$ composition of xylem water, ‰ VSMOW.
ε	light conversion efficiency, mg J^{-1}.
ε_d	full kinetic fractionation in the soil pores, ‰.
$\varepsilon_{d,\mathrm{eff}}$	effective isotopic fractionation during CO_2 diffusion in soil pores, ‰.
$\varepsilon_{\mathrm{eq}}$	water equilibrium fractionation, ‰.
$\varepsilon_{k,c}$	CO_2 canopy-scale kinetic fractionation factor for $C^{18}OO$, ‰.
$\varepsilon_{k,w}$	canopy-scale kinetic fractionation factor for $H_2{}^{18}O$, ‰.
θ_a	proportion of soil pores filled with air, $m^3\,m^{-3}$.
θ_{eq}	CO_2 hydration efficiency.
θ_{sat}	the soil water content at saturation, $m^3\,m^{-3}$.
θ_t	total CO_2 porosity, $m^3\,m^{-3}$.
θ_w	soil water content, $m^3\,m^{-3}$.
ρ_a	air density, kg m^{-3}.
Φ_M	stability function.
Γ	CO_2 compensation point, mg m^{-3}.

Acknowledgments

Funding for this research was provided by the Natural Science and Engineering Research Council. The first author acknowledges funding by the Brazilian National Council for Scientific and Technological Development (CNPq). Xuhui Lee was supported by the US National Science Foundation (grant ATM-0914473) and the Ministry of Education of China (grant PCSIRT). We would also like to thank the two anonymous reviewers for their insightful suggestions.

References

Allison, C. A., R. J. Francey, and H. A. J. Meijer (1995), Recommendations for the reporting of stable isotope measurements of carbon and axygen in CO_2 gas. Reference and Intercomparison Materials for Stable Isotopes of Light Elements, *IAEA-TECDOC*, *825*, 155–162.

Amundson, R., L. Stern, T. Baisden, and Y. Wang (1998), The isotopic composition of soil and soil-respired CO_2, *Geoderma*, *82*, 83–114.

Bird, R. B., W. E. Stewart, and E. N. Lightfoot (2002), *Transport Phenomena*, 2nd ed., 895 pp., John Wiley, New York.

Bowen, G. J., and J. Revenaugh (2003), Interpolating the isotopic composition of modern meteoric precipitation, *Water Resour. Res.*, *39*(10), 1299, doi:10.1029/2003wr002086.

Bowling, D. R., P. P. Tans, and R. K. Monson (2001), Partitioning net ecosystem carbon exchange with isotopic fluxes of CO_2, *Global Change Biol.*, *7*(2), 127–145.

Bowling, D. R., S. D. Sargent, B. D. Tanner, and J. R. Ehleringer (2003), Tunable diode laser absorption spectroscopy for stable isotope studies of ecosystem-atmosphere CO_2 exchange, *Agric. For. Meteorol.*, *118*(1–2), 1–19.

Bowling, D. R., D. E. Pataki, and J. T. Randerson (2008), Carbon isotopes in terrestrial ecosystem pools and CO_2 fluxes, *New Phytol.*, *178*(1), 24–40.

Brenninkmeijer, C. A. M., P. Kraft, and W. G. Mook (1983), Oxygen isotope fractionation between CO_2 and H_2O, *Isot. Geosci.*, *1*(2), 181–190.

Calvet, J. C., V. Rivalland, C. Picon-Cochard, and J. M. Guehl (2004), Modelling forest transpiration and CO_2 fluxes—Response to soil moisture stress, *Agric. For. Meteorol.*, *124*(3–4), 143–156.

Cosby, B. J., G. M. Hornberger, R. B. Clapp, and T. R. Ginn (1984), A statistical exploration of the relationships of soil-moisture characteristics to the physical-properties of soils, *Water Resour. Res.* , *20*(6), 682–690, doi:10.1029/WR020i006p00682.

Craig, H., and L. I. Gordon (1965), Deuterium and oxygen-18 variations in the ocean and the marine atmosphere, in *Stable Isotopes in Oceanographic Studies and Paleotemperatures*, edited by E. Tongiorgi, pp. 9–130, Lab. di Geol. Necl, Pisa, Italy.

Cuntz, M., J. Ogee, G. D. Farquhar, P. Peylin, and L. A. Cernusak (2007), Modelling advection and diffusion of water isotopologues in leaves, *Plant Cell Environ.*, *30*(8), 892–909.

Dongmann, G., H. W. Nurnberg, H. Forstel, and K. Wagener (1974), Enrichment of $H_2{}^{18}O$ in leaves of transpiring plants, *Radiat. Environ. Biophys.*, *11*(1), 41–52.

Dubbert, M., M. Cuntz, A. Piayda, C. Maguas, and C. Werner (2013), Partitioning evapotranspiration—Testing the Craig and Gordon model with field measurements of oxygen isotope ratios of evaporative fluxes, *J. Hydrol.*, *496*, 142–153.

Ehleringer, J. R., and C. B. Osmond (1989), Stable isotopes, in *Plant Physiological Ecology: Field Methods and Instrumentation*, edited by R. W. Pearcy et al., pp. 289–300, Chapman and Hall, London.

Farquhar, G. D., and L. A. Cernusak (2005), On the isotopic composition of leaf water in the non-steady state, *Funct. Plant Biol.*, *32*(4), 293–303.

Farquhar, G. D., and J. Lloyd (1993), Carbon and oxygen isotope effects in the exchange of carbon dioxide between terrestrial plants and the atmosphere, in *Stable Isotopes and Plant Carbon-Water Relations*, edited by J. R. Ehleringer, A. E. Hall, and G. D. Farquhar, pp. 47–70, Academic Press, San Diego.

Farquhar, G. D., J. Lloyd, J. A. Taylor, L. B. Flanagan, J. P. Syvertsen, K. T. Hubick, S. C. Wong, and J. R. Ehleringer (1993), Vegetation effects on the isotope composition of oxygen in atmospheric CO_2, *Nature*, *363*(6444), 439–443.

Ferrio, J. P., M. Cuntz, C. Offermann, R. Siegwolf, M. Saurer, and A. Gessler (2009), Effect of water availability on leaf water isotopic enrichment in beech seedlings shows limitations of current fractionation models, *Plant Cell Environ.*, *32*(10), 1285–1296.

Flanagan, L. B., J. P. Comstock, and J. R. Ehleringer (1991), Comparison of modeled and observed environmental-influences on the stable oxygen and hydrogen isotope composition of leaf water in *Phaseolus vulgaris* L, *Plant Physiol.*, *96*(2), 588–596.

Flanagan, L. B., J. R. Brooks, G. T. Varney, and J. R. Ehleringer (1997), Discrimination against $C^{18}O^{16}O$ during photosynthesis and the oxygen isotope ratio of respired CO_2 in boreal forest ecosystems, *Global Biogeochem. Cycles*, *11*(1), 83–98, doi:10.1029/96GB03941.

Flexas, J., M. Ribas-Carbo, A. Diaz-Espejo, J. Galmes, and H. Medrano (2008), Mesophyll conductance to CO_2: Current knowledge and future prospects, *Plant Cell Environ.*, *31*(5), 602–621.

Gillon, J., and D. Yakir (2001), Influence of carbonic anhydrase activity in terrestrial vegetation on the ^{18}O content of atmospheric CO_2, *Science*, *291*(5513), 2584–2587.

Griffis, T. J. (2013), Tracing the flow of carbon dioxide and water vapor between the biosphere and atmosphere: A review of optical isotope techniques and their application, *Agric. For. Meteorol.*, *174–175*, 85–109.

Griffis, T. J., X. Lee, J. M. Baker, S. D. Sargent, and J. Y. King (2005), Feasibility of quantifying ecosystem-atmosphere $C^{18}O^{16}O$ exchange using laser spectroscopy and the flux-gradient method, *Agric. For. Meteorol.*, *135*(1–4), 44–60.

Griffis, T. J., X. Lee, J. M. Baker, K. Billmark, N. Schultz, M. Erickson, X. Zhang, J. Fassbinder, W. Xiao, and N. Hu (2011), Oxygen isotope composition of evapotranspiration and its relation to C-4 photosynthetic discrimination, *J. Geophys. Res.*, *116*, doi:10.1029/2010JG001514.

Hesterberg, R., and U. Siegenthaler (1991), Production and stable isotopic composition of CO_2 in a soil near Bern, Switzerland, *Tellus Ser. B-Chem. Phys. Meteorol.*, *43*(2), 197–205.

Jacobs, C. M. J. (1994), Direct impact of atmospheric CO_2 enrichment on regional transpiration, PhD thesis, 179 pp., Wageningen Agricultural University, Wageningen.

Keenan, T., S. Sabate, and C. Gracia (2010), The importance of mesophyll conductance in regulating forest ecosystem productivity during drought periods, *Global Change Biol.*, *16*(3), 1019–1034.

Lai, C. T., J. R. Ehleringer, B. J. Bond, and K. T. Paw U (2006), Contributions of evaporation, isotopic non-steady state transpiration and atmospheric mixing on the $\delta^{18}O$ of water vapour in Pacific Northwest coniferous forests, *Plant Cell Environ.*, *29*(1), 77–94.

Lee, X. H., K. Kim, and R. Smith (2007), Temporal variations of the $^{18}O/^{16}O$ signal of the whole-canopy transpiration in a temperate forest, *Global Biogeochem. Cycles*, *21*, GB3013, doi:10.1029/2006GB002871.

Lee, X. H., T. J. Griffis, J. M. Baker, K. A. Billmark, K. Kim, and L. R. Welp (2009), Canopy-scale kinetic fractionation of atmospheric carbon dioxide and water vapor isotopes, *Global Biogeochem. Cycles*, *23*, GB1002, doi:10.1029/2008GB003331.

Majoube, M. (1971), Oxygen-18 and deuterium fractionation between water and steam, *J. Chim Phys. Phys.-Chim. Biol.*, *68*, 1423–1436.

Ogee, J., Y. Brunet, D. Loustau, P. Berbigier, and S. Delzon (2003), MuSICA, a CO_2, water and energy multilayer, multileaf pine forest model: Evaluation from hourly to yearly time scales and sensitivity analysis, *Global Change Biol.*, *9*(5), 697–717.

Ogée, J., P. Peylin, M. Cuntz, T. Bariac, Y. Brunet, P. Berbigier, P. Richard, and P. Ciais (2004), Partitioning net ecosystem carbon exchange into net assimilation and respiration with canopy-scale isotopic measurements: An error propagation analysis with $^{13}CO_2$ and $CO^{18}O$ data, *Global Biogeochem. Cycles*, *18*, GB2019, doi:10.1029/2003GB002166.

Riley, W. J., C. J. Still, B. R. Helliker, M. Ribas-Carbo, and J. A. Berry (2003), ^{18}O composition of CO_2 and H_2O ecosystem pools and fluxes in a tallgrass prairie: Simulations and comparisons to measurements, *Global Change Biol.*, *9*(11), 1567–1581.

Ronda, R. J., H. A. R. De Bruin, and A. A. M. Holtslag (2001), Representation of the canopy conductance in modeling the surface energy budget for low vegetation, *J. Appl. Meteorol.*, *40*(8), 1431–1444.

Santos, E., C. Wagner-Riddle, X. Lee, J. Warland, S. Brown, R. Staebler, P. Bartlett, and K. Kim (2012), Use of the isotope flux ratio approach to investigate the $C^{18}O^{16}O$ and $^{13}CO_2$ exchange near the floor of a temperate deciduous forest, *Biogeosciences*, *9*(7), 2385–2399.

Saxton, K. E., and P. H. Willey (2006), The SPAW model for agricultural field and pond hydrologic simulation, in *Watershed Models*, edited by D. K. Frevert and V. P. Singh, pp. 401–435, CRC Press, Boca Raton, Fla.

Seibt, U., L. Wingate, J. Lloyd, and J. A. Berry (2006), Diurnally variable $\delta^{18}O$ signatures of soil CO_2 fluxes indicate carbonic anhydrase activity in a forest soil, *J. Geophys. Res.*, *111*, G04005, doi:10.1029/02006JG000177.

Skirrow, G. (1975), The dissolved gases: Carbon dioxide, in *Chemical Oceanography*, edited by J. P. Riley and G. Skirrow, pp. 1–92, Academic Press, San Diego, Calif.

Song, X., M. M. Barbour, G. D. Farquhar, D. R. Vann, and B. R. Helliker (2013), Transpiration rate relates to within- and across-species variations in effective path length in a leaf water model of oxygen isotope enrichment, *Plant Cell Environ.*, *36*(7), 1338–1351.

Stern, L. A., R. Amundson, and W. T. Baisden (2001), Influence of soils on oxygen isotope ratio of atmospheric CO_2, *Global Biogeochem. Cycles*, *15*(3), 753–759, doi:10.1029/2000GB001373.

Still, C. J., et al. (2009), Influence of clouds and diffuse radiation on ecosystem-atmosphere CO_2 and $CO^{18}O$ exchanges, *J. Geophys. Res.*, *114*, G01018, doi:10.1029/2007JG000675.

Sturm, P., W. Eugster, and A. Knohl (2012), Eddy covariance measurements of CO_2 isotopologues with a quantum cascade laser absorption spectrometer, *Agric. For. Meteorol.*, *152*, 73–82.

Tans, P. P. (1998), Oxygen isotopic equilibrium between carbon dioxide and water in soils, *Tellus Ser. B-Chem. Phys. Meteorol.*, *50*(4), 163–178.

Teklemariam, T., R. M. Staebler, and A. G. Barr (2009), Eight years of carbon dioxide exchange above a mixed forest at Borden, Ontario, *Agric. For. Meteorol.*, *149*(11), 2040–2053.

Weiss, R. F. (1974), Carbon dioxide in water and seawater: The solubility of a non-ideal gas, *Mar. Chem.*, *2*(3), 203–215.

Welker, J. M. (2000), Isotopic ($\delta^{18}O$) characteristics of weekly precipitation collected across the USA: An initial analysis with application to water source studies, *Hydrol. Processes*, *14*(8), 1449–1464.

Welp, L. R., X. Lee, K. Kim, T. J. Griffis, K. A. Billmark, and J. M. Baker (2008), $\delta^{18}O$ of water vapour, evapotranspiration and the sites of leaf water evaporation in a soybean canopy, *Plant Cell Environ.*, *31*(9), 1214–1228.

Welp, L. R., X. Lee, T. J. Griffis, X.-F. Wen, W. Xiao, S. Li, X. Sun, Z. Hu, M. V. Martin, and J. Huang (2012), A meta-analysis of water vapor deuterium-excess in the midlatitude atmospheric surface layer, *Global Biogeochem. Cycles*, *26*, GB3021, doi:10.1029/2011GB004246.

Werner, C., et al. (2012), Progress and challenges in using stable isotopes to trace plant carbon and water relations across scales, *Biogeosciences*, *9*(8), 3083–3111.

Wingate, L., U. Seibt, K. Maseyk, J. Ogee, P. Almeida, D. Yakir, J. S. Pereira, and M. Mencuccini (2008), Evaporation and carbonic anhydrase activity recorded in oxygen isotope signatures of net CO_2 fluxes from a Mediterranean soil, *Global Change Biol.*, *14*(9), 2178–2193.

Wingate, L., et al. (2009), The impact of soil microorganisms on the global budget of $\delta^{18}O$ in atmospheric CO_2, *Proc. Natl. Acad. Sci. U.S.A.*, *106*(52), 22,411–22,415.

Wingate, L., J. Ogee, R. Burlett, and A. Bosc (2010), Strong seasonal disequilibrium measured between the oxygen isotope signals of leaf and soil CO_2 exchange, *Global Change Biol.*, *16*(11), 3048–3064.

Xiao, W., X. Lee, T. J. Griffis, K. Kim, L. R. Welp, and Q. Yu (2010), A modeling investigation of canopy-air oxygen isotopic exchange of water vapor and carbon dioxide in a soybean field, *J. Geophys. Res.*, *115*, G01004, doi:10.1029/02009JG001163.

Xiao, J., et al. (2011), Assessing net ecosystem carbon exchange of US terrestrial ecosystems by integrating eddy covariance flux measurements and satellite observations, *Agric. For. Meteorol.*, *151*(1), doi:10.1016/j.agrformet.2010.09.002.

Xiao, W., X. Lee, X. Wen, X. Sun, and S. Zhang (2012), Modeling biophysical controls on canopy foliage water ^{18}O enrichment in wheat and corn, *Global Change Biol.*., *18*(5), 1769–1780.

Yakir, D., and L. D. L. Sternberg (2000), The use of stable isotopes to study ecosystem gas exchange, *Oecologia*, *123*(3), 297–311.

Yakir, D., and X. F. Wang (1996), Fluxes of CO_2 and water between terrestrial vegetation and the atmosphere estimated from isotope measurements, *Nature*, *380*(6574), 515–517.